INTERNATIONAL JOURNAL OF CLIMATOLOGY RMetS Royal Meteorological Society

Climate reconstruction over southern Altai mountains and Dzungarian region, Central Asia based on tree-rings since 1650

Journal:	*International Journal of Climatology*
Manuscript ID	JOC-17-0379
Wiley - Manuscript type:	Research Article
Date Submitted by the Author:	18-May-2017
Complete List of Authors:	Byambaa, Oyunmunkh; University of Bonn, Meteorological Institute Weijers, Stef; University of Bonn, Department of Geography Löffler, Jörg; Univ Bonn, Germany, Department of Geography Suran, Byambagerel; National University of Mongolia, Department of Environmental Sciences and Forest Engineering, School of Engineering and Applied Sciences Nergui, Soninkhishig; National University of Mongolia, Department of Biology, School of Sciences and Arts Buerkert, Andreas; University Kassel, Faculty of Organic Agricultural Science Goenster-Jordan, Sven; University Kassel, Faculty of Organic Agricultural Science Simmer, Clemens; University of Bonn, Meteorological Institute
Keywords:	climate variation and change, global warming, little ice age, Mongolia, temperature, precipitation, larix sibirica, Indian summer monsoon intensification

Climate reconstruction over southern Altai mountains and Dzungarian region, Central Asia based on tree-rings since 1650

Byambaa Oyunmunkh, Stef Weijers, Joerg Loeffler, Suran Byambagerel, Nergui Soninkhishig, Andreas Buerkert, Sven Goenster-Jordan, and Clemens Simmer*

We reconstruct summer temperature and precipitation over the cold and arid Altai-Dzungarian region for the period 1650-2012 by from tree-ring chronologies. Besides the corroboration of some results from previous studies, regionally specific variabilities and changes are observed both for the Little Ice Age and the 20th century. Remarkable is a late 20th century wetting trend probably connected to the intensification of the hydrological cycle accompanying global warming.

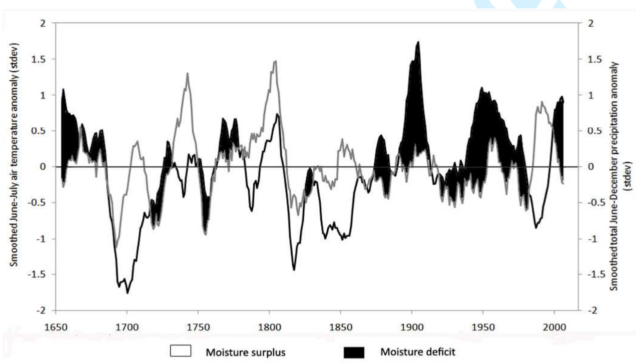

11-year running mean of reconstructed mean June-July temperature (black line) and June-December precipitation sum anomalies (grey line) (normalized by the 1650-2012 mean). Moisture deficit and surplus periods of 363 year climate variations over Altai-Dzungarian region are suggested by overlapping reconstructed precipitation and air temperature.

Title page

Title: Climate reconstruction over southern Altai mountains and Dzungarian region, Central Asia based on tree-rings since 1650

Names of authors:

Byambaa Oyunmunkh[1], Stef Weijers[2], Joerg Loeffler[2], Suran Byambagerel[3], Nergui Soninkhishig[3], Andreas Buerkert[4], Sven Goenster-Jordan[4], and Clemens Simmer[1*]

Affiliations:

[1]Meteorological Institute, University Bonn, Germany

[2]Department of Geography, University Bonn, Germany

[3]National University of Mongolia, Mongolia

[4]Faculty of Organic Agricultural Science, University Kassel, Germany

*Corresponding author:

Clemens Simmer

Meteorological Institute, University Bonn

Auf dem Huegel 20, D-53121 Bonn, Germany

E-mail: csimmer@uni-bonn.de

Abstract

This research focused on climate reconstruction based on tree rings in order to understand long-term climatic variation and change over the Altai-Dzungarian region, which may help to estimate the effects of global warming on future water availability in this region. We found that slope aspect in the southern Altai mountains significantly influences tree growth response to climate, despite sampling of hypothetically temperature-sensitive upper tree-line forests. Upper tree-line growth on a north-facing slope was found to be limited by air temperature variability, while growth on a north-west facing slope was found to be limited by precipitation. We were able to reconstruct June-July air temperatures for the period 1450-2012 and June-December precipitation sums for the period 1650-2012 based on tree ring-width chronologies from Siberian larch (*Larix sibirica* Ledeb.) from two sites in the southern Altai mountains, Mongolia. This area is representative for the cold-arid Altai-Dzungarian region, which is weakly influenced by both mid-latitude and tropical climate systems. The temperature and precipitation reconstructions explain 43.6% and 52.5% of the variance during the observation period (1977-2012), respectively. The reconstructions show a gradual increase in precipitation since 1930, and maxima warm periods in 20th century. The area apparently has become drier since 1875 with the 20th century characterized by frequent warm and dry summers, while the Little Ice Age (1650-1874) was marked by overall wet alternating cold and warm episodes. Our findings also reveal a late 20th century cool and wet period over Altai mountains, which is already observed across other mountainous areas of China and Nepal, most probably caused by the Indian Summer Monsoon intensification. This could be an indication for the intensification of the hydrological cycle as a result of global warming. The 21st century will likely stay warm

and dry unless unforeseen feedbacks in the climate system change this trend.

Keywords: Temperature; Precipitation; Climatic variation and change; Global warming; Little Ice Age, Mongolia; *Larix sibirica;* Indian Summer Monsoon intensification

1 Introduction

The Altai mountain range lies in the cross-border region of Kazakhstan, China, Mongolia and Russia. The vegetation zones of this region follow moisture and temperature gradients, with a decrease in moisture and an increase in temperature from North to South and from West to East (Zhang *et al.*, 2015). The Dzungarian semi-desert basin is bounded by the Altai mountains in the north and the Tian Shan mountains in the south. The lack of long-term instrumental observations from such outback desert and mountain areas hinder the estimation of climate dynamics and change in these regions. Schwikowski *et al.* (2009) suggested that climate proxies based on tree rings, relict wood, lake sediments and glaciers, which often can be found in these remote regions in rather undisturbed states, should be used for exploring climate change and variability. Accordingly, tree rings from the Altai mountain range are widely used as climate proxies to reconstruct past variability and changes of temperature, precipitation and drought in Mongolia, China, and Russia. Panyushkina *et al.* (2005), for example, studied the decadal variability of Siberian larch (*Larix sibirica*) tree ring-widths from upper tree-line sites in the Russian southeast Altai. They found growth differences between trees from glacier-free and glacier-occupied valleys during three periods as a result of glacier dynamics while both groups showed an increase in June-July temperature from 1890 until the 1950s and a cooling afterwards. A July and August temperature reconstruction based on tree ring oxygen and carbon isotopes of Siberian pine (*Pinus sibirica* Du Tour) from the central part of the Russian Altai by Loader *et al.* (2010) revealed a similar variability with warming from 1870 to 1950 and cooling until the 1980s, in accordance with June-July temperature reconstructions from Siberian larch over the Altai mountains in China and east Kazakhstan by Chen *et al.* (2012) and Zhang *et al.* (2015). Chen *et al.* (2014) reported a 20th century wetting trend in a tree-ring-based reconstruction of June-July precipitation for the southern Chinese Altai. Davi *et al.* (2009) found a regional scale increase in the growing season moisture availability (June-September) for the Mongolian Altai throughout both the 20th and 21st century, which has not been observed in tree ring chronologies from central and eastern Mongolia. Most chronologies show similar overall trends, but differ in the higher frequency variability as a result of the heterogeneous climate of the Altai mountains. Moreover, PAGES 2k Consortium (2013) described that continental-scale temperature variability reconstructions from multi proxy data for the reason that all reconstructions showed no globally synchronous warm and cold episodes except generally cold conditions between AD 1580 and 1880 during the past two millennia and past global climate change occurred distinctly different over region by region. The area-weighted average of past estimated temperature from all continents illustrates that the warmest period occurred in late 20th century between 1971 and 2000 (PAGES, 2013). However, according to temperature reconstruction from Arctic, although 20th century is the warmest period, the period of 1941 to 1970 was warmer than the estimated warmest period from all regions (PAGES, 2013), which is similar to reconstructed summer temperature pattern over Altai mountains (Panyushkina *et al.*, 2005; Loader *et al.*, 2010; Chen *et al.*, 2012; Zhang *et al.*, 2015). Also, Shi *et al.* (2015) investigated the spatial and temporal evolution of summer temperature in eastern and south central Asia using multi-proxy records and defined the warmest period in Asia was late 20th century but the warming in the 20th century shows from east to west temperature gradient due to climate of Asia influenced by local factors including Tibetan Plateau and complex monsoon systems, which affects the stability of climatic teleconnections. Both these regional temperature reconstructions (PAGES, 2013; Shi *et al.*, 2015) agree Altai mountain region could have different past temperature variability and change pattern from the Northern Hemisphere temperature pattern. Hence, it is interesting to understand local scale climate variability and change response to global warming, which is important for human society.

The winter climate of the continental and arid Altai-Dzungarian region (AD) in the southern Altai mountain range is characterized by the prevailing thermal Siberian High Pressure System, which directs dry and cold arctic air masses to the region.

During the warm summers local precipitation is generated from humid air masses originating either from the Atlantic Ocean or from southwesterly monsoonal airflow, and no single flow system clearly dominates the climate. Weak influences of many systems, like the East Asian Monsoon, the Indian Summer Monsoon, the North Pacific High, and even El Niño/Southern Oscillation also exist (Pederson *et al.*, 2001; Schwikowski *et al.*, 2009). Due to these many influences and the different sensitivities of these systems to global climate change, the attribution of summer climate change in this region is challenging.

This paper aims to investigate long-term climate dynamics and trends over the AD through reconstructing climate variability over the past centuries based on tree ring chronologies from two upper tree-line forest patches in the southern Altai mountains: one growing on a north- and the other on a northwest-facing slope. It was hypothesized that tree growth response to climate at upper tree lines of both north and northwest aspect would be controlled by temperature variability of the growing season. In contrast, however, growth on the north-facing slope was found to be predominantly temperature limited, while growth on the northwest-facing slope was found to be precipitation limited. Hence, we developed separate transfer function models for summer air temperature and precipitation against tree ring-growth through calibration with weather data from a close-by climate station. Furthermore, we identified past warm/cold and wet/dry climate episodes over the entire period with both reconstructed temperature and precipitation data (363 years; 1650-2012).

2 Material and methods

2.1 Tree-ring data

In the southern part of the Mongolian Altai mountains (Figure 1) patches of Siberian larch forest are often found on north- and northwest-facing slopes. Although previous research on external disturbances in Larch Forests of the Mongolian Altai by Dulamsuren and Khishigjargal (2012), have mentioned that the area is too cold for insect outbreaks, forests in the Mongolian Altai have been subjected to extensive logging in 20th century. Two sampling sites (Khargait and Khets), both with rather steep slopes (25-33˚), were selected based on site conditions free of fire and insect effects, and minimum human disturbances, as derived from interviews with local officers and site inspection. Local people of the southern Mongolian Altai mountains asserted that the main disturbance in this area has been intensive logging from the 1960s to 1990s, and that in recent decades no widespread fires have occurred. Still, some forest patches have experienced limited fire due to drought in 1973-1975 and 2008-2009, but our sampling sites have not been affected.

The Khargait site, located on a north-facing slope, is characterized by large boulders covered by a thin soil layer and alpine shrubs, while the Khets site, located on a northwest-facing slope, has a well-developed soil layer with grasses and young trees. In July 2014, we took 32 cores from 17 and 46 cores from 23 trees from these sites, respectively. Except for two trees, two cores were taken from each tree, from opposite sides, perpendicular to the slope direction.

The cores of each site were marked with calendar dates and visually cross-dated using so-called pointer years, which are isolated years with exceptionally narrow or wide ring widths. During cross-dating, the tree ring-width series were scanned carefully for potential missing and false rings. By matching tree-ring width patterns among cores and examining the ring structure (Fritts, 1976), a site chronology with agreement among growth sequence of trees is derived and compared to all cores in order to detect missing, partial and false rings formed under severe conditions. The tree ring-widths were measured to the nearest 0.001 mm with a Velmex measuring system and MeasureJ2X software (Velmex, Inc). Measurement accuracy and visual cross-dating among chronologies at each site were checked by statistical cross-dating in COFECHAv6.06 program, which calculates Pearson correlation coefficients between segments of individual ring-width series with a master chronology consisting of all other series at the dated position and ten positions forward and backward (Grissino-Mayer, 2001). Flagged, i.e. potentially incorrectly dated segments, were checked and corrected when missing or false rings in that ring-width series were found. Tree ring-width series were standardized by a conservative negative exponential or a straight-line fit using the ARSTAN for Windows (version ARS41c_xp) software (Cook *et al.*, 2006) to remove effects of aging and non-climatic factors in the series (Cook, 1985).

The climate signal strength in a site chronology and its reliability are described by mean sensitivity, expressed population signal (EPS), and mean correlation between tree-ring series (Rbar). The mean sensitivity is the relative difference between adjacent ring widths, which ranges from 0 (no difference) to higher values and indicates the range of year to year variations in radial growth in response to climate (Fritts, 1976). The EPS quantifies the strength of the common signal for a set of tree-ring series in a given chronology (Cook and Kairiukstis, 1990, Wigley *et al.*, 1984), and is based on Rbar and sample size. Wigley *et al.* (1984) suggested 0.85 as a lower acceptable threshold for the EPS. The Rbar is a measure for the common growth signal or variance between all trees. We calculated running Rbar and EPS in ARSTAN among all tree-ring series used for each chronology in 50 year intervals with 25 years overlap.

The oldest parts of the site chronologies with low sample depth and EPS<0.85, which are segment of 1402-1449 with 6 cores of the Khargait chronology and segment of 1569 and 1649 with 8 cores of the Khets were excluded from analysis and reconstruction in order to reduce uncertainty and apply constructive length of these chronologies to climate reconstruction.

2.2 Climate station data

Duchinjil (1951 m above sea level (a.s.l)) is the nearest climate station located approx.

36-40 km away from the sampling sites. The observations at this station were selected for the reconstruction of summer air temperature and precipitation based on the tree ring-width chronologies. More distant climate stations such as Baitag (1186 m a.s.l) and Qinghe (1463 m a.s.l.,China) were not used for reconstruction due to significantly lower climate-ring width correlations. At Duchinjil, 55% of the total annual precipitation, which was 129±33 mm in the period of 1977-2012, falls in summer months of June, July, and August, while winter months (December, January and February) contribute only 6% on average to the annual sum, although much larger contributions may occur occasionally (Figure 2a). Since July precipitation is the highest, which is typical for Mongolia and Inner Mongolia, the interannual variability of July precipitation is often used to quantify precipitation variation in this region (Iwao, 2006). Mean monthly air temperatures fluctuate from –22.0°C in January to +15.8°C in July at Duchinjil (Figure 2b).

Temperature and precipitation trends at Duchinjil (Figure 3) suggest a rapid summer (MJJA) warming since 1994 and drying since 1998, which potentially led to an increase in the occurrence of moisture deficit conditions.

2.3 Regression model development for summer air temperature and precipitation reconstruction

We used DendroClim2002 (Biondi and Waikul, 2004) to estimate the effect of monthly climate variables on tree ring width for the time period of available instrumental climate data. DendroClim2002 uses 1000 bootstrapped samples to compute Pearson's correlation and response function coefficients as multivariate estimates derived from a principal component regression model. Significances were tested at the $p<0.05$ level. An 18-month window of climate data from May of the prior year through October of the current year was compared with the detrended tree ring width chronologies.

In the correlation and response function analyses, prior year precipitation (at Khets) and current year air temperature (at Khargait) were identified as main drivers of radial growth and were applied to a transfer function model development for each respective site chronology. Since the station record is relatively short and because of the overall warming trend during the observation period, the entire time series was needed for calibration and verification of the temperature transfer function model. The leave-one-out cross validation method was therefore used (Michaelsen, 1987); 33 of the complete 36 years were used for calibration and one year for validation of the goodness-of-fit of a total of 36 models. To avoid autocorrelation in model validation, both adjacent years of the one validation year were excluded. The model, which exhibited the lowest Root Mean Square Error (RMSE), was selected for the final reconstruction of the climate record and related statistics.

As there was no trend in the instrumental precipitation record, we used two separate periods for calibration (1977-1996) and verification (1997-2012) to calculate the precipitation transfer function model skill statistically. In a principal component regression analysis, a 362-year precipitation reconstruction was produced with a transfer function model using the June-December precipitation sum as a predictand, and previous and current year tree-ring width of the Khets chronology as predictors.

For the verification of the derived transfer function models we used statistics common in dendrochronology, such as Pearson's correlation coefficient (r), Coefficient of Determination (R^2), Reduction of Error (RE), Coefficient of Efficiency (CE), Product Mean (PM) test, and first difference sign test (Cook *et al.*, 1999; Weijers *et al.*, 2010). The association between tree rings and climate is measured by r while the percent of variance in climate explained by ring-widths is evaluated by R^2. RE and CE quantify model skill for climate reconstruction from the tree rings and range between minus infinity and one; positive values close to 1 indicate good skill and negative values a lower skill than climatology (Cook *et al.*, 1999; Fritts, 1976; Weijers *et al.*, 2010). The PM test (Fritts, 1976) takes into account both the sign and magnitude of the actual and estimated departure from the mean values, while the non-parametric first difference sign test uses only the sign of change to quantify similarities between two series.

To examine the spatial scale of the reconstructions, the spatial correlation was calculated between the reconstructions and the gridded CRU TS 3.23 dataset available (0.5x0.5°resolution) over the period 1977-2012. The CRU data set is produced by the Climate Research Unit at the University of East Anglia (Harris and Jones, 2015); we used the KNMI climate explorer (http://climexp.knmi.nl) for this analysis.

3 Results and Discussion

3.1 Site chronology and climate-growth response

Site chronologies for Khargait and Khets show relatively high mean sensitivity values of 0.299 and 0.318, respectively, when compared to some previous studies from the

Altai mountains (0.27, Davi *et al.*, 2009; 0.181-0.266, Chen *et al.*, 2014; 0.174-0.198, Chen *et al.*, 2012, respectively; Grissino-Mayer, 2001). First order autocorrelations of Khargait and Khets chronologies have decreased from 0.72 to 0.57 and from 0.76 to 0.62, respectively after standardization by ARSTAN. The EPS statistic, a measure of chronology reliability, ranges between 0.94 and 0.99 for Khargait and between 0.95 and 0.99 for Khets over the entire period, which is above the accepted threshold of 0.85 (Wigley *et al.*, 1984). The running mean correlation coefficients among the tree ring series in a chronology (Rbar) for 50-year intervals with 25-year overlap, range from 0.45 to 0.77 for both site chronologies (Table 1).

Low precipitation and high temperature are growth controlling climate factors, which affect soil moisture, the water balance of trees, tree respiration and photosynthesis, and evapotranspiration (Fritts, 1966). Aspect of slope is the most crucial site factor in growth response than elevation and latitude (Fritts, 1976). Moreover, Fritts (1976) reports that topography affects water balance and energy by controlling the amount of radiation received by the site and by influencing the amount and allocation of moisture. The Khargait sampling site, which is located on a north-facing slope at high elevation and contains big boulders, receives less incident radiation. In contrast, the Khets site, which is located on a north-west facing slope and is thus prone to westerly winds, receives more radiation and may thus be drier (lower soil moisture content), and has a fine developed soil. The two chronologies are positively correlated ($r=0.35$, $p<0.05$) but growth at the sites was found to be driven by different climate factors. Tree ring formation of Siberian larch at high elevations in the Altai mountains starts in May by cell division and lengthening, and ceases in August by thickening of tracheid cell walls

(Chen *et al.*, 2012). Hence, we tested correlations between the site chronologies and both monthly mean air temperature and precipitation sums.

The Khargait chronology correlated positively with mean June–August temperatures ($r=0.27$ to 0.34, $p<0.05$) prior to the year of growth, with mean May-August temperatures ($r=0.23$ to 0.64, $p<0.05$) of the current year, and with previous year August precipitation sums ($r=0.21$, $p<0.05$), as well as with those of January ($r=0.29$, $p<0.05$) and March ($r=0.21$, $p<0.05$) of the current year (Figure 4a). The chronology was negatively correlated with October precipitation both of the prior ($r=-0.23$, $p<0.05$) and of the current year ($r=-0.22$, $p<0.05$). The response function coefficients indicate a significant tree ring-width response to the current year mean June temperatures ($r=0.42$, $p<0.05$) and October precipitation sums ($r=-0.26$, $p<0.05$; Figure 4b). Overall, mean monthly temperatures correlated more strongly with the chronology than precipitation sums. We developed a summer temperature transfer function model based on the Khargait chronology and average June-July temperatures, as excluding August temperatures slightly improved the model performance ($r=0.63$ instead of 0.61, $p<0.05$). Our results corroborate findings from previous studies in the Chinese southern Altai mountain range by Chen *et al.* (2012), Zhang *et al.* (2015) and Wang *et al.* (2013), who showed positive correlations of tree ring widths with June-July air temperatures. Higher June-July temperatures may increase radial growth both through an acceleration of photosynthesis as well as through higher soil moisture content due to increased snowmelt.

For the Khets chronology positive correlations (Figure 4c) were found with mean monthly precipitation sums of July until December of the prior year ($r=0.20$ to 0.39, $p<0.05$) except October ($r=0.04$) and of the current year for July and August ($r=0.22$ and 0.27, respectively; $p<0.05$). The chronology correlated negatively with mean January temperature ($r=-0.30$, $p<0.05$) of the current year. The response function coefficients showed a significant growth response to monthly precipitation sums of July until November of the prior year ($r=0.21$ to 0.32, $p<0.05$) except October ($r=-0.02$; Figure 4d). These findings are partly in line with Chen *et al.* (2014) who identified that the radial growth of Siberian spruce in southern Altai mountains (China) is positively correlated with July-August and winter precipitation (especially December), and May-July precipitation of current year. Fritts (1974) stated that growth of arid-site conifers during the current year might be enhanced by above-average precipitation in late summer and early autumn of the previous year due to its promotion of carbohydrate storage and bud formation. Furthermore, winter precipitation, which mostly falls as snow from November to March in our research area, may increase soil moisture content during the early growing season due to snowmelt. More precipitation falls in November and December compared to the period January to March at Duchinjil (Figure 2a), which may explain the positive correlations found with November and December precipitation sums. The previous year June through December precipitation sum showed a stronger correlation ($r=0.636$, $p<0.01$) with the Khets chronology than the previous year summer precipitation sum (June to August; $r=0.592$, $p<0.01$) alone. Thus, we have chosen to reconstruct June-December precipitation sums.

In summary, the Khargait chronology was used for the reconstruction of mean summer (June-July) temperature for the period 1450-2012, and the Khets chronology for the reconstruction of total summer through early winter precipitation for the period 1650-2012.

3.2 Summer air temperature reconstruction

Our reconstructed summer temperature series explains 43.6% of the year-to-year variance of the instrumental observations and contains the same general positive trend (Figure 5). The transfer function model validation statistics (Table 2) indicate, with positive values of RE and PM, and significant first-difference sign test, that our temperature reconstruction captures the high frequency variation of instrumental data well.

According to our 562-year June-July temperature reconstruction based on the Khargait chronology, mean summer temperatures ranged from 12.4 to 16.6°C over the period 1450-2012, which does not exceed the summer temperature variability observed at Duchinjil over the period 1977-2012 (Figure 6).

Particularly warm decades are suggested for the periods 1880-1910 and 1940-1975 and cold periods for 1680-1710 and 1810-1860. These cold periods and cooling in 1930s are also revealed by a 750-year high resolution temperature reconstruction (1250-2000) from ice core oxygen isotope record from the Belukha glacier in the Siberian Altai and explained as periods of solar low activity (Eichler *et al.*, 2009; Schwikowski *et al.*, 2009). Moreover, periods of volcanic activity induced cooling (Briffa *et al.*, 1998; Eichler *et al.*, 2009) and periods of low solar activity (Schwikowski *et al.*, 2009) coincide with our periods with low temperatures in our temperature reconstruction

(Figure 6). Most cool summers are observed during the period of low solar activity and explosive volcanic eruptions. Likewise, Eichler *et al.* (2009) found a strong correlation between solar activity and temperature variations for the period 1250-1850 in the Altai region with a 10-30 year lag temperature response due to indirect mechanisms between solar activity and climate. During the industrial period of 1850-2000 the greenhouse gas CO_2 concentration shows a significant correlation with regional temperature variation, while solar forcing contribution decreased.

The clear warming trend in the late 20th century follows a cooler period between 1983-1998, which was also reflected in tree ring chronologies from mountainous areas in Nepal, and China and explained by an increased Indian Summer Monsoon intensity (Braeuning and Mantwill, 2004; Wang *et al.*, 2013; Zhang *et al.*, 2015). Chen (2012) related this cooling to enhanced cloudiness and rainfall over the Altai mountains leading to wetter and cooler conditions causing reduced growth of *Larix sibirica* at the treeline.

Our findings agree largely with the decadal variability of June and July temperature from a larch tree-ring chronology obtained from the Russian southeast Altai (Panyushkina *et al.*, 2005), with the July and August temperature variability obtained from Siberian Pine (*Pinus sibirica*) trees growing on north facing slopes in the central part of the Russian Altai (Loader *et al.*, 2010), with June-to-July temperature reconstructions from Siberian Larch (*Larix sibirica*) over the Altai mountains in China and Kazakhstan (Chen *et al.*, 2012; Zhang *et al.*, 2015), and with an August and September temperature reconstruction based on spruce, fir and larch from north facing slopes of the Tibetan plateau (Braeuning and Mantwill, 2004). There are, however, differences in the degree of variation in the 17th and 18th century, and the short cooling period in the early 20th century was only observed by Braeuning and Mantwill (2004), Panyushkina *et al.* (2005), and Zhang *et al.* (2015). In Braeuning and Mantwill's study (2004) deviations of individual chronology for the northeastern part of Tibetan plateau from the regional trend were explained as a result of the influence of different monsoonal air masses on the temperature at the treeline.

The cooling trends in the early 17th, early 18th, and mid-19th century visible in our June-July temperature reconstruction (Figure 6) were also observed in earlier studies for northern Mongolia by Davi *et al.* (2015) and D' Arrigo *et al.* (2000, 2001). Davi *et al.* (2015) reconstructed June-July temperatures from 931 to 2005 from Siberian larch growing at Ondor Zuun Nuruu located west of Lake Hovsgol, approx. 800 km from our research area, through calibration with climate records from four stations in Russia and Mongolia. D'Arrigo *et al.* (2000, 2001) estimated July and August temperatures for the period from 450 to 1738 for northern Mongolia using climate records from the Irkutsk station in Russia. The cooling trend over northern Mongolia from these studies is greater in the early 1600s compared to the one in the early 1700s, while it is smaller in the early 1600s than in the early 1700s in our findings.

Our reconstruction and other studies for the southern Mongolian Altai do not indicate a continuous 20th century warming trend as observed in the Northern Mongolia reconstructions (Davi *et al.*,2015; D' Arrigo *et al.*, 2000, 2001; Davi *et al.*, 2015), but a decrease in summer temperatures starting in the 1950s followed by a steep rise in the 1990s. This rapid warming over Mongolia slowed down temporarily since 2002 probably following a natural global climate variability caused by a redistribution of heat in the ocean, volcanic eruptions, the recent minimum in the 11 year solar cycle, and the decadal cooling caused by La Niña in the Pacific Ocean (Dagvadorj *et al.*, 2014). La Niña and El Niño-Southern Oscillation (ENSO) may have an impact on Mongolian climate, as Davi et al (2010) found 2-7 year periodicities in the ENSO range from spatially averaged drought reconstruction for Mongolia, which are weakly negatively correlated with each other, due to the long distance to oceans and potential for influence by other forcings. Conversely, the Altai mountainous area showed wetter than average phases during extreme summer droughts (1999-2002) in Mongolia. Davi *et al.* (2009) noted that large scale climate modes like ENSO are only vaguely present in tree-ring records from Western Mongolia. Still, during warm ENSO phases strengthened southwesterlies have brought humid air masses from the Indian and western Pacific Oceans and enhanced precipitation in southwest Central Asia in autumn and spring of recent decades, while during the La Niña cooling phases this moisture flux decreased and leading to drought in Central Asia (Mariotti, 2007). Overland *et al.* (2015) suggested that the persistent weather conditions with frequent extreme weather events including severe winters and blockings (Greenland and Ular-Siberia) since 2007 are caused by a slower development of large amplitude planetary waves.

3.2 Precipitation reconstruction

The precipitation reconstruction explains 61.9% of the variance in the instrumental data during the calibration period, and high positive RE, CE and PM suggest a high reliability of the model (Table 3). The correlation between reconstructed and instrumental data over the whole common period is 0.72 ($p<0.01$) and the model explains 52.25% of the variance in the observations (Figure 7). The reconstructed precipitation variability for the time period 1650 to 2012 shows a gradual trend towards wetter conditions since 1930, interspersed with wet maxima in the 1950s (1956 to 1961) and 1990s (1989-1996)(Figure 8).

The period between 1840 and 1930 was characterized by relatively small variations, while the centuries before this period (late 1600s to early 1800s) were characterized by much stronger variations. Extreme variation of precipitation in the 1700s and the wettest two periods in the 1900s in our findings are supported by Davi *et al.* (2009), who described the periods 1957-1961 and 1993-1996 as the wettest five year periods according to a reconstruction of the June to September PDSI (Palmer Drought Severity Index) obtained from Siberian larch chronologies from 1565 to 2004 in the northwestern Altai mountains, Mongolia, which were calibrated with monthly 2.5°x 2.5° PDSI grid cell data. Also, Chen *et al.* (2014) revealed two similar wet periods (1956-1962 and1985-2006) in their June-July precipitation reconstruction for the Chinese southern Altai mountains.

Davi *et al.* (2009) and Chen *et al.* (2014) show a slight wetting since the 1880s and moderate wetting between the 1980s and 2000. The latter wetting trend was supported by an instrumental data analysis for northwestern China by Shi *et al.* (2006) and for western Mongolia by Dagvadorj *et al.* (2014). While all reconstructions in this region agree on the overall trend, there are differences in the high frequency variation of precipitation. These differences might be explained by regional orographic effects of the Altai mountains which may result in complex interactions with the storm tracks bringing rain to this region (Davi *et al.*, 2009).

Davi *et al.* (2010) reported a significant correlation between increasing precipitation from the Indian Summer Monsoon and the reconstructed drought variability obtained from a tree-ring network over Mongolia (r=0.50 over the period 1951-1993, and 0.36 over 1900-1993), which is in line with our results for the southern Altai. Also Braeuning and Mantwill (2004), Wang *et al.* (2013), and Chen (2012) explained this wetting trend as a consequence of an increasing Indian Summer Monsoon intensity over some mountainous areas in the northern hemisphere. Instrumental data analyses from northwestern China and Mongolia confirm, that the climate in this area changed from a warm and dry to warm and wet between 1987 and 1999 due to enhanced southerly winds, which carry more water vapor from the Indian Ocean to the north (Shi *et al.*, 2006; Dagvadorj *et al.*, 2014). In addition Chen *et al.* (2014) suggested that the wetting trend over the Southern Altai in northwest China in the 1980s could be explained by increased strength of westerlies related to a warming of sea surface temperatures over the North Atlantic and Indo-West Pacific Oceans (Chen *et al.*, 2013). Chen *et al.* (2013) reconstructed PDSI for Western Tian Shan, Central Asia, which is located in southwest margin of Dzunagrian Basin, and found that regional moisture variability is connected to the westerly circulation, especially of southwesterly and tropical ocean-atmosphere systems. In addition, Gong and Ho (2002) reported a warming and wetting trend across continental Asia from the late 1970s to the 1990s, however, especially during winter, and a weakening northerly and northeasterly wind over East Asia due to a weakening of the dry and cold Siberian Highin parallel to a pressure reduction over the Atlantic ocean and high-mid latitude Asia. Later Jeong *et al.* (2011) found that the intensity of the Siberian High has increased back during the past two decades accompanied by an increase of Eurasian winter snow cover since around 2000 (Estilow *et al.*, 2015) and a near surface cooling over the center of the Siberian High.

3.3 Spatial correlations of reconstructed air temperature and precipitation

The correlation between reconstructed and gridded instrument-based mean June-July temperature for the period 1977-2012 demonstrates that our temperature reconstruction contains a regional signal covering the Altai and western Sayan mountains, northern Mongolia ($r=0.6$, $p<0.1$), the Mongolian Plateau ($r=0.5$, $p<0.1$), and the Dzungarian Basin ($r=0.2$-0.6 related to distance from Altai mountain range, $p<0.1$, Figure 9a). The recorded mean June-July temperature at Duchinjil station reflects an even larger area covering the entire Altai-Dzungarian region and Mongolia in the same correlation range ($r=0.6$, $p<0.1$, Figure 9b).

Reconstructed and instrument-based gridded total June to December precipitation from 1977 to 2012 are only weakly correlated ($r=0.2$, $p<0.1$) at the local scale over the southwestern Altai mountains and parts of Dzungarian Basin in China (Figure 9c). This fine-scale variability of the precipitation signal in this complex mountainous terrain was verified by the relatively high spatial correlation ($r=0.2$-0.5, $p<0.1$) in this area between observed total June-December precipitation at Duchinjil station and the gridded data (Figure 9d).

Overall, while our reconstructed summer temperature variability characterizes a regional scale climate signal, the reconstructed precipitation related more to the local scale water availability.

3.4 Reconstructed climate variation

The combined 363-year reconstructions of precipitation and summer temperature anomalies over AD (Figure 10) indicate that frequent warm and moisture deficit summers have replaced the more common cold/warm moisture surplus episodes of the Little Ice Age (1650-1874) with the exception of some dry years since 1875 and a short cold and wet period between 1980 and 2000.

In total, the moisture deficit phases (1650-1690, 1715-1730, 1750-1780, 1830-1835) during the Little Ice Age (LIA) lasted 104 years, and only 35 percent of this, in total, 225 years long period can be characterized as warm and dry as the 20th century. Between 1875 and 2012, 85% of the years have experienced moisture deficit, and 70% of last 137 years were warm and dry. Thus, warm and dry years have increased since 1875.

According to Putnam *et al.* (2016), wetter climate conditions during the LIA (defined as the period between 1150 and 1845) can be inferred from geomorphological, biological, and historical evidence found in the Tarim Basin, which neighbors the Dzungarian Basin. During that period, northern hemisphere mountain glaciers expanded as a reaction to the lower temperatures and snowlines. In addition, the Tarim Basin became wetter and a deeper snowpack over high mountains was accumulated due to increasing orographic precipitation as a result of a southward shift or strengthening of the boreal westerlies to the interior Asian desert belt. Putnam *et al.*(2016) suggest that the drying over inner Asia throughout the 20th century might have led to a northward migration of westerlies accompanied by a northward expansion of deserts. Based on an ice-core record from the Altai region, Schwikowski *et al.* (2009) and Eichler*et al.* (2009) suggested that solar forcing was the main driving force for the temperature variation in this area from 1250 to 1850. Spatial and temporal patterns of surface temperatures during the LIA (defined as 1450-1850) were characterized by orbital, solar and volcanic forcing and by internal variability (Masson-Delmotte *et al.*, 2013). Masson-Delmotte *et al.* (2013) suggested that the change of incoming solar radiation due to variations of the Earth's orbital parameters and its axial tilt, could have caused the cooling trend of the past 5000 years over the mid to high latitudes of the northern hemisphere, which has reversed into a warming trend since the 20th century. Finally, the grand solar minima (low solar activity) associated with cold conditions between 1645 and 1715 and a long-term increasing trend in solar activity in the early 20th century together with internal variability, volcano eruption, and the anthropogenic increase of greenhouse gases contributed to this global surface temperature fluctuation (Eichler *et al.*, 2009, Masson-Delmotte *et al.*, 2013).

4 Summary and conclusions

Tree ring proxies from the southern Altai mountains, Mongolia, were used to reconstruct mean June-July temperatures (1450-2012) and June-December precipitation sums (1650-2012) for the Altai-Dzungarian region. The reconstructed air temperatures and precipitation sums explained 43.6% and 52.5%, respectively, of the variance in climate data measured at the weather station nearest to the sampling sites. Our temperature reconstruction reflects a broader-scale variability over AD and northern Mongolia than our precipitation reconstruction; the latter represents finer scale variability confined to a part of the AD only, due to the complex mountainous terrain. On the longer time scale of each reconstruction, wetting trend and maxima warm periods are observed over AD since 1930 and 1875, respectively. According to the 363-year combined reconstructed climate anomalies, AD was wetter during the Little Ice Age and drier throughout the 20th century, which is in line with findings for the neighboring Tarim Basin. A short cooling and wetting period was observed in the late 20th century, which was likely a result of a weakening of the high pressure system and an increase of the Indian Summer Monsoon intensity. This period was followed by an abrupt warming and a slight drying in the early 21th century over AD.

Authors' contribution

BO carried out the fieldwork with the assistance of NS, AB, and SG. Laboratory analysis and interpretation of the results was done with the help of SW, JL, and SB. The manuscript was prepared and compiled by BO and CS. All authors reviewed the manuscript and significantly contributed with comments and additions.

Acknowledgements

This research was supported by the WATERCOPE project, funded by the International Fund for Agricultural Development (IFAD) [grant number I-R-1284]. We thank Prof.Dr. Baatarbileg Nachin for technical support at the Tree Ring Laboratory of the National University of Mongolia, Batbold Gantumur for field sampling and

Gombo Sainbayar for assisting in laboratory work.

References

D' Arrigo R, Jacoby G, Pederson N, Frank D, Buckley B, Nachin B, Mijiddorj R, Dugarjav Ch. 2000. Mongolian tree-rings, temperature sensitivity and reconstructions of Northern Hemisphere temperature. *The Holocene* **10 (6):** 669-672

D' Arrigo R, Jacoby G, Pederson N, Frank D, Buckley B, Nachin B, Mijiddorj R, Dugarjav Ch. 2001. 1738 years of Mongolian temperature variability inferred from a tree-ring width chronology of Siberian Pine. *Geophysical Research Letters* **28 (3):** 543-546

Briffa K, Jones P, Schweingruber F, Osborn T. 1998. Influence of volcanic eruptions on Northern Hemisphere summer temperature over the past 600 years, *Nature* **393:** 450–455.

Biondi F, Waikul K. 2004. DENDROCLIM2002: a C++ program for statistical calibration of climate signals in tree-ring chronologies. *Computer & Geosciences* **30:** 301-311

Braeuning A, Mantwill B. 2004. Summer temperature and summer monsoon history on the Tibetan Plateau during the last 400 years recorded by tree rings. *Geophysical Research Letters* **31:** doi:10.1029/2004GL020793.

Cook ER. 1985. *A time series analysis approach to Tree ring standardization.* The University of Arizona. Arizona.

Cook ER, Kairiukstis LA. 1990. *Methods of Dendrochronology*. Applications in the Environmental Sciences. Kluwer Academic Press, Dordrecht.

Cook ER, Meko DM, Stahle DW, Cleaveland MK. 1999. Drought Reconstruction for the Continental United States. *Journal of Climate* **12:** 1145-1162

Cook ER, Krusic PJ. 2006. *Program ARSTAN*. A Tree-Ring Standardization Program Based on Detrending and Autoregressive Time Series Modeling, with Interactive Graphics. Tree-Ring Laboratory. Lamont Doherty Earth Observatory of Columbia University. Palisades. New York

Chen F, Yuan YJ, Wei WS, Zhang TW. 2014. Precipitation reconstruction for the southern Altay Mountains (China) from tree rings of Siberian spruce, reveals recent wetting trend. *Dendrochronologia* **32:** 266-272

Chen F, Yuan YJ, Chen FH, Wei WS, Yu SL, Chen XJ, Fan ZA, Zhang RB, Zhang TW, Shang HM, Qin L. 2013. A 426-year drought history for Western Tian Shan, Central Asia inferred from tree-rings and its linkages to the North Atlantic and Indo-West Pacific Oceans. *The Holocene* **23:** 1095-1104

Chen F, Yuan YJ, Wei WS, Fan ZA, Zhang TW, Shanh HM, Zhang RB, Yu SL, Ji CR, Qin Li. 2012. Climate response of ring width and maximum latewood density of Larix sibirica in the Altay mountain reveals recent warming trend. *Annals of Forest Science*. doi:10.1007/s13595-013-0187-2.

Dagvadorj D, Batjargal Z, Natsagdorj L. 2014. *Mongolia second assessment report on climate change - 2014*. Ministry of Environment and Green Development of Mongolia. Ulaanbaatar, Mongolia.

Davi NK, Jacoby GC, D' Arrigo RD, Baatarbileg N, Li J, Curtis AE. 2009. A tree-ring-based drought index reconstruction for far-western Mongolia: 1565-2004, *International Journal of Climatology* **29:** 1508-1514. doi:10.1002/joc.1798.

Davi N, Jacoby G, Fang K, Li J, D' Arrigo R, Baatarbileg N, Robison D. 2010. Reconstructing drought variability for Mongolia based on a large scale tree ring network: 1520-1993. *Journal of Geophysical Research* **115:** D22103, doi:10.1029/2010JD013907.

Davi NK, D' Arrigo R, Jacoby GC, Cook ER, Anchukaitis KJ, Nachin B, Rao MP, Leland C. 2015. A long-term context (931-2005 C.E.) for rapid warming over Central Asia. *Quaternary Science Reviews* **121:** 89-97. doi:10.1016/j.quascirev.2015.05.020.

Dulamsuren Ch, Khishigjargal M. 2012. Opposing growth trends created by external disturbance in larch forests of the Mongolian Altai. *Exploration into the Biological Resources of Mongolia (Halle/Saale)* ***12*****:** 353–363.

Eichler A, Olivier S, Henderson K, Laube A, Beer J, Papina T, Gäggeler HW, Schwikowski M. 2009. Temperature response in the Altai region lags solar forcing. *Geophysical Research Letters* **36:** L01808, doi:10.1029/2008GL035930.

Estilow TW, Young AH, Robinson DA. 2015. A long-term Northern Hemisphere snow cover extent data record for climate studies and monitoring. *Earth System Science Data* **7:** 137-142, doi:10.5194/essd-7-137-2015.

Fritts HC. 1966. Growth-Rings of Trees: Their correlation with climate. *Journal of Science*: 973-979. doi: 10.1126/science.154.3752.973.

Fritts HC. 1974. Relationships of Ring Widths in Arid-Site Conifers to Variations in Monthly Temperature and Precipitation. *Ecological Monographs* **44:** 411–440. doi: 10.2307/1942448

Fritts HC. 1976. *Tree rings and Climate*. Academic Press. London.

Frank D, Ovchinnikov D, Kirdyanov A, Esper J. 2007. TRACE - Tree Rings in Archaeology, Climatology and Ecology, Vol. 5: Proceedings of the DENDROSYMPOSIUM 2006, April 20th – 22nd 2006, Tervuren, Belgium.

Schriften des Forschungs zentrums Jülich, Reihe Umwelt **74:** 85 - 96.

Grissino-Mayer HD. 2001. Evaluating crossdating accuracy: A manual and tutorial for the computer program COFECHA. *Tree-Ring Research* **57 (2):** 205-221.

Gong DY, Ho CH. 2002. The Siberian High and climate change over middle to high latitude Asia. *Theoretical and Applied Climatology* **72:** 1-9.

Harris IC, Jones PD. 2015. *CRU TS3.23: Climatic Research Unit (CRU) Time-Series (TS) Version 3.23 of High Resolution Gridded Data of Month-by-month Variation in Climate (Jan. 1901- Dec. 2014)*. Centre for Environmental Data Analysis, University of East Anglia Climatic Research Unit; *09 November 2015*. doi:10.5285/4c7fdfa6-f176-4c58-acee-683d5e9d2ed5.

Iwao K, Takahashi M. 2006. Interannual change in summer time precipitation over northeast Asia. *Geophysical Research Letter* **33:** L16703. doi:10.1029/2006/GL027119.

Jeong JH, Ou T, Linderholm HW, Kim BM, Kim SJ, Kug JS, Chen D. 2011. Recent recovery of the Siberian High intensity, *Journal of Geophysical Research* **116:** D23102. doi:10.1029/2011JD015904.

Loader NJ, Helle G, Los SO, Lehmkuhl F, Schleser GH. 2010. Twentieth-century summer temperature variability in the southern Altai Mountains: A carbon and oxygen isotope study of tree rings. *The Holocene* **20 (7):** 1149-1156. doi:10.1177/0959683610369507.

Mariotti A. 2007. How ENSO impacts precipitation in southwest central Asia. *Geophysical Research Letters* **34:** doi:10.1029/2007GL030078.

Masson-Delmotte V, Schulz M, Abe-Ouchi A, Beer J, Ganopolski A, Gonzalez Rouco JF, Jansen E, Lambeck K, Luterbacher J, Naish T, Osborn T, Otto-Bliesner B, Quinn T, Ramesh R, Rojash M, Shao X, Timmermann A. 2013. *Information from Paleoclimate Archives. In: Climate change 2013:* The Physical Science Basis. Contribution of Working Group I to the Fifth Assessment Report of the Intergovernmental Panel on Climate Change [Stocker, T.F., D.Qin, G.-K. Plattner, M. Tignor, S.K. Allen, J. Boschung, A. Nauels, Y. Xia, V. Bexaand P.M. Midgley (eds.)]. Cambridge University Press, Cambridge, United Kingdom and New York, NY, USA.

Michaelsen J. 1987. Cross-validation in statistical climate forecast models. *Journal of Climate and Applied Meteorology* **26:** 1589-1600.

Overland J, Francis JA, Hall R, Hanna E, Kim SJ, Vihma T. 2015. The melting arctic and mid-latitude weather patterns: Are they connected? *Journal of Climate* **28 (20):** 7917-7932. doi:10.1175/JCLI-D-14-00822.1.

PAGES 2k Consortium (2013) Continental-scale temperature variability during the past two millennia. *Nature Geoscience* **6(5):** 339-346. doi: 10.1038/NGEO1797

Panyushkina IP, Ovtchinnikov DV, Adamenko MF. 2005. Mixed response of decadal variability in larch tree-ring chronologies from upper tree-lines of the Russian Altai. *Tree-ring research* **61 (1):** 33-42.

Pederson N, Jacoby GC, D'Arrigo RD, Cook ER, Buckley BM, Dugarjav Ch, Mijiddorj R. 2001. Hydrometeorological Reconstruction for Northeastern Mongolia Derived from Tree Rings: AD1651-1995. *Journal of Climate* **14:** 872-881.

Putnam AE, Putnam DE, Andreu-Hayles L, Cook ER, Palmer JG, Clark EH, Wang Ch, Chen F, Denton GH, Boyle DP, Bassett SD, Birkel SD, Martin-Fernandez J, Hajdas I, Southon J, Garner ChB, Cheng H, Broecker WS. 2016. Little Ice Age wetting of Interior Asian deserts and the rise of the Mongol Empire. *Quaternary Science*

Reviews **131:** 33-50. doi:10.1016/j.quascirev.2015.10.033.

Schwikowski M, Eichler A, Kalugin I, Ovtchinnikov D, Papina T. 2009. Past climate variability in the Altai. *Pages News* **17 (1):** 44-45

Shi F, Ge Q, Yang B, Li J, Yang F, Ljungqvist FCh, Solomina O, Nakatsuka T, Wang N, Zhao S, Xu Ch, Fang K, Sano M, Chu G, Fan Z, Gaire NP, Zafar MU. 2015. A multi-proxy reconstruction of spatial and temporal variations in Asian summer temperatures over the last millennium. *Climate change* **131 (4):** 663. doi:10.1007/s10584-015-1413-3

Shi Y, Shen Y, Kang E, Li D, Ding Y. 2006. Recent and future climate change in northwest China. *Climate change* **80:** 379. doi:10.1007/s10584-006-9121-7.

Wang H, Chen F, Yuan Y, Yu S, Shang H, Zhang T. 2013. Temperature signals in tree-ring width chronology of alpine treeline conifers from the Baishui River Nature Reserve China. *Terrestrial, Atmospheric and Oceanic Sciences* **24:** 887-898, doi:10.3319/TAO.2013.06.18.01(A).

Wigley TML, Briffa KR, Jones PD. 1984. On the average value of correlated time series, with applications in dendroclimatology and hydrometeorology. *Journal of Applied Meteorology* **25:** 201-213.

Weijers S, Broekman R, Rozema J. 2010. Dendrochronology in the High Arctic: July air temperatures reconstructed from annual shoot length growth of the circumarctic dwarf shrub Cassiopetetragona. *Quaternary Science Reviews* **29:** 3831–3842. doi:10.1016/j.quascirev.2010.09.003.

Zhang T, Yuan Y, Hu Y, Wei W, Shang H, Huang L, Zhang R, Chen F, Yu Sh, Fan Z, Qin L. 2015. Early summer temperature changes in the southern Altai Mountains of Central Asia during the past 300 years. *Quaternary International* **358:** 68-76.

doi:10.1016/j.quaint.2014.12.005.

Tables

Table 1: Sampling sites and standardized ring-width chronology information and statistics

Tree ring sites	**Khargait**	**Khets**
Latitude (N)	46°39'	46° 43'
Longitude (E)	91°26'	91° 31'
Elevation (m)	2748	2603
Slope aspect	North	Northwest
No of cores	32	46
Chronology period	1402-2013, 612	1569-2013, 445
Period, number of years with EPS>0.85	1450-2013, 564	1650-2013, 364
First-order autocorrelation	0.57	0.62
Average mean sensitivity[a]	0.299	0.318
EPS[b]	0.94-0.99	0.95-0.99
Rbar[c]	0.45-0.75	0.46-0.77

[a]Average mean sensitivity and first order autocorrelation of standardized chronology (Cook and Krusic, 2006) [b]Expressed population signal (Wigley *et al.*, 1984)

[c]Rbar - the mean correlation coefficient among all tree-ring series used in a chronology

Table 2: Statistics of the leave-one-out validation results for the transfer function model of the June-July mean temperature reconstruction with the Khargait chronology over the common period 1977-2012

r	R^2	AdjR^2	RE	Sign test	Product mean test
0.657**	0.436	0.415	0.382	27+/9-**	0.304*

r - Pearson's correlation coefficient, $\mathbf{R^2}$– Coefficient of Determination, **Adj**$\mathbf{R^2}$ – Adjusted for degrees of freedom, **RE**- Reduction of error statistic, **- $p<0.01$ * $p<0.05$

Table 3: Calibration and verification statistics of June-December precipitation sum reconstruction from the Khets tree-ring width chronology

	Calibration (1977-1996)	Verification (1997-2012)	Calibration (1997-2012)	Verification (1977-1996)	Full calibration (1977-2012)
r	0.787***	0.642**	0.488*	0.637**	0.72**
R^2	0.619***		0.238*		0.52**
AdjR^2	0.575***		0.184*		0.51**
RE	0.620	0.294	0.238	0.432	
CE	0.620	0.266	0.238	0.417	
Sign test	16+/4-**	11+/5-	11+/5-	16+/4-**	24+/12-
Products means test	602**	492**	150*	345**	

r - Pearson's correlation coefficient, **R^2**– Coefficient of Determination, **AdjR^2** – Adjusted for degrees of freedom, **RE**- Reduction of error statistic, **CE**- Coefficient of Efficiency

*** $p<0.001$ **$p<0.01$ * $p<0.05$

Figure legends

Figure 1: Map of the Altai-Dzungarian region in Central Asia. The white stars indicate the locations of the climate stations near the two larch (*Larix sibirica*) sampling sites, shown as white diamonds. The black areas indicate lakes and the grey scale indicates elevation from low ranges by dark color to high, mountain ranges by white color.

Figure 2: Distribution of climate data shown in Box-Whiskers. Interquantile range, median, and spread of data are illustrated by box, thick line, and whiskers, respectively. Outliers are marked by open circles. a: Mean monthly precipitation sums (mm) and b. Mean monthly air temperatures (˚C) observed at Duchinjil station over the period of 1977-2012.

Figure 3: Time series of temperature and precipitation anomalies at Duchinjil averaged for the period May to August. Shown are anomalies normalized by the respective standard deviations and smoothed by 5 year running mean. Moisture deficit and surplus summer conditions are described by coinciding relative higher air temperature and lower precipitation, and relative lower air temperature and higher precipitation, respectively.

Figure 4: Pearson's correlation coefficients and standardized response function coefficients between tree ring width chronologies of Khargait (a, b), and Khets (c, d) and the monthly mean air temperature and precipitation sums as measured at Duchinjil station of a 18 months window from May prior to and ending in October of the year of growth over the period 1977-2012. Both values are obtained by simple correlation and partial regression. The standardized response function coefficients were obtained by dividing the partial regression coefficients by their standard deviations for 1000

bootstraps (Biondi and Waikul, 2004). Values greater than |0.2| are significant at $p<0.05$.

Figure 5: Mean June-July air temperature estimated from Khargait larch ring-widths (grey line) and observed data (black line) at Duchinjil station over the 1977-2012. The Pearson's correlation coefficient ($r=0.64$, $p<0.01$) between estimated and observed June-July temperature is significantly positive.

Figure 6: Tree ring based mean June-July air temperature reconstruction (thin grey line) and 11-year (thick dark grey line) low-pass filtered curve, along with mean (dashed line), and observation (black line). The horizontal thin and thick grey lines indicate the range of one and two standard deviations, respectively. The below horizontal black line shows the number of cores used for the ring-width chronology. Grey bars show periods of low solar activity (S = Spörer, M = Maunder, D = Dalton and G = Gleissberg minima) (Schwikowski *et al.*, 2009) and triangles indicate volcanic eruptions (Briffa *et al.*, 1998; figure by Eichler *et al.*, 2009).

Figure 7: June-December precipitation sums estimated from Khets larch ring-widths (grey line) and observed data (black line) at Duchinjil station over the period 1977-2012. The Pearson's correlation coefficient ($r= 0.72$, $p<0.01$) between estimated and observed June-December precipitation sums is significantly positive.

Figure 8: Tree-ring based reconstruction of June to December precipitation sums (thin grey line) and 11-year (thick dark grey line) low-pass filtered curve, along with mean (dashed line), and observations (black line). The horizontal thin and thick grey lines indicate the range of one and two standard deviations, respectively. The horizontal black line below shows the number of cores used for the ring-width chronology.

Figure 9: Spatial correlation maps showing the correlations between the gridded CRU TS 3.23 (0.5˚x0.5˚) climate dataset and the reconstructed and observed air temperature and precipitation at Duchinjil station over the period of 1977-2012 using the KNMI climate explorer (http://climexp.knmi.nl). The black star and diamond indicate the locations of the climate station and sampling site, respectively. a. gridded and reconstructed June to July averaged temperature, b. gridded and observed June to July averaged temperature, c. gridded and reconstructed June to December precipitation sums, d. gridded and observed June to December precipitation sums

Figure 10: Smoothed (11-year running mean), reconstructed mean June-July temperature (black line) and June-December precipitation sum anomalies (grey line) (normalized by the 1650-2012 mean). Moisture deficit and surplus periods of 363 year climate variations over Altai-Dzungarian region are suggested by overlapping reconstructed precipitation and air temperature.

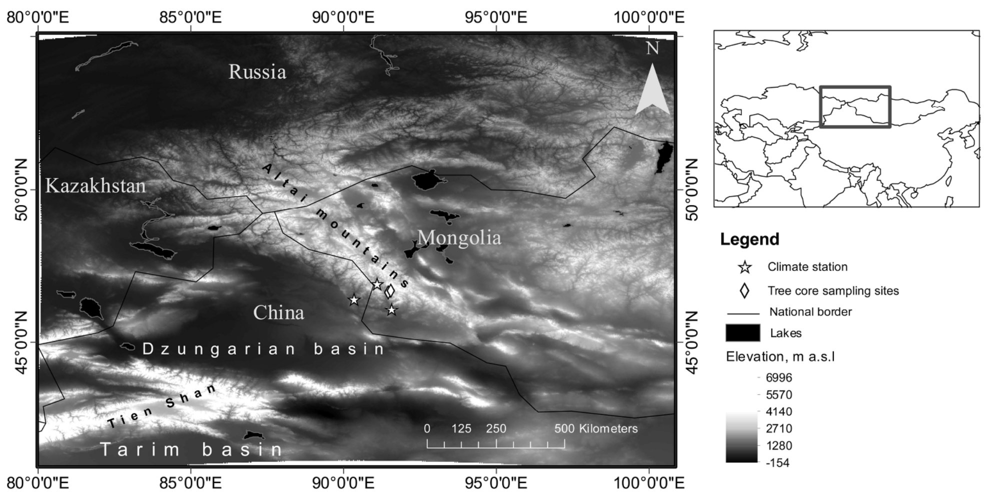

Figure 1

210x148mm (300 x 300 DPI)

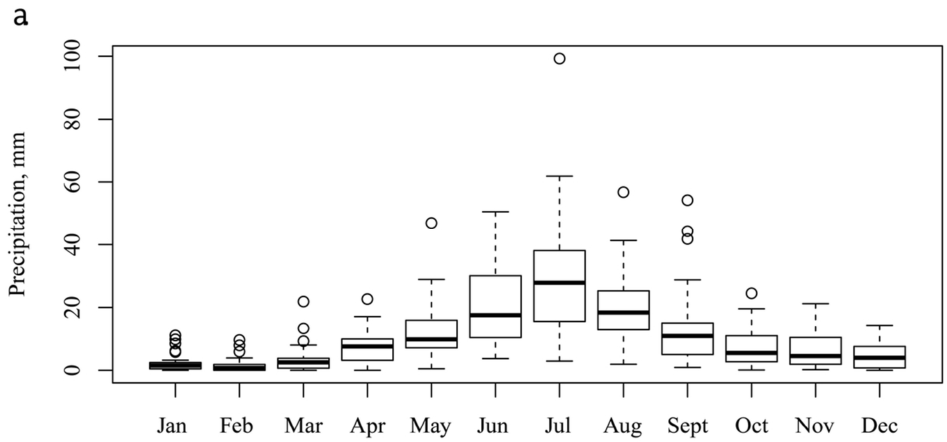

Figure 2a

108x64mm (300 x 300 DPI)

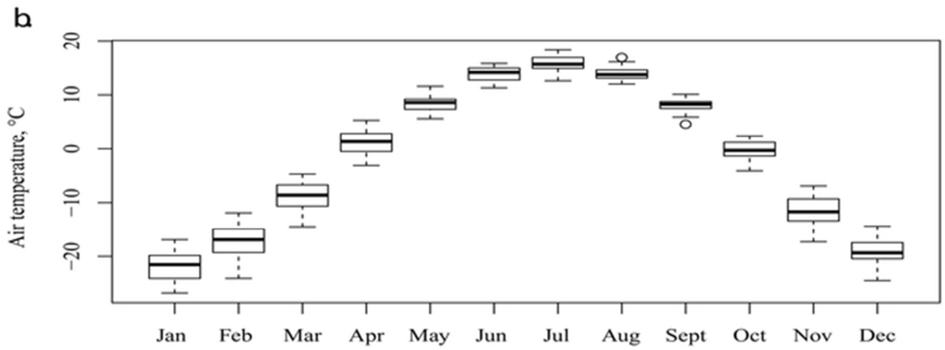

Figure 2b

59x27mm (300 x 300 DPI)

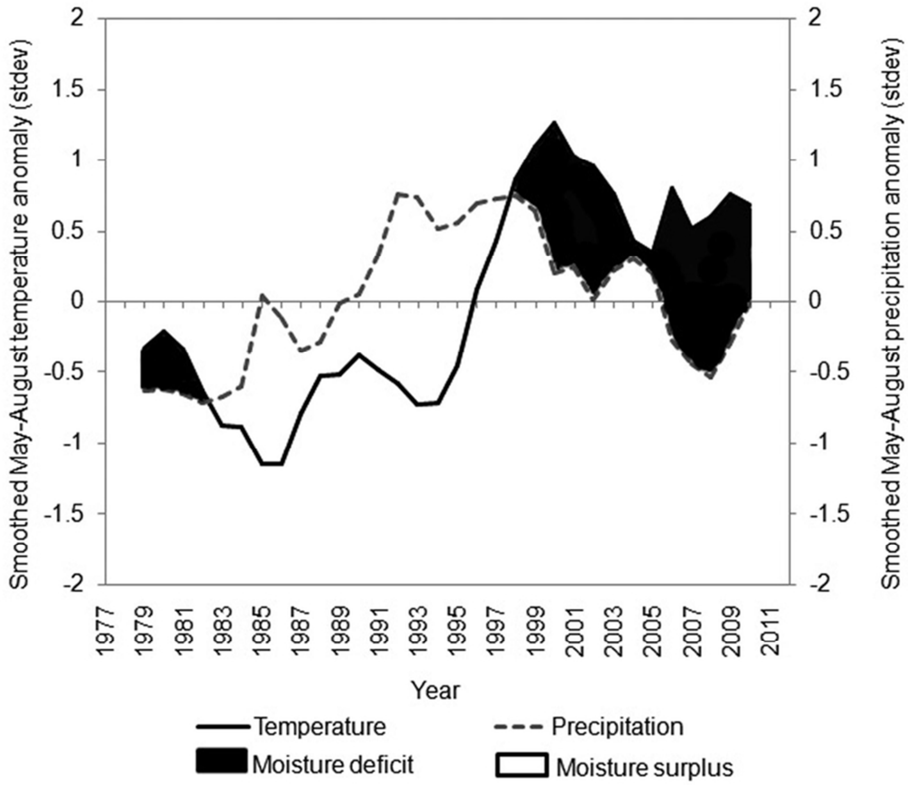

Figure 3

77x67mm (300 x 300 DPI)

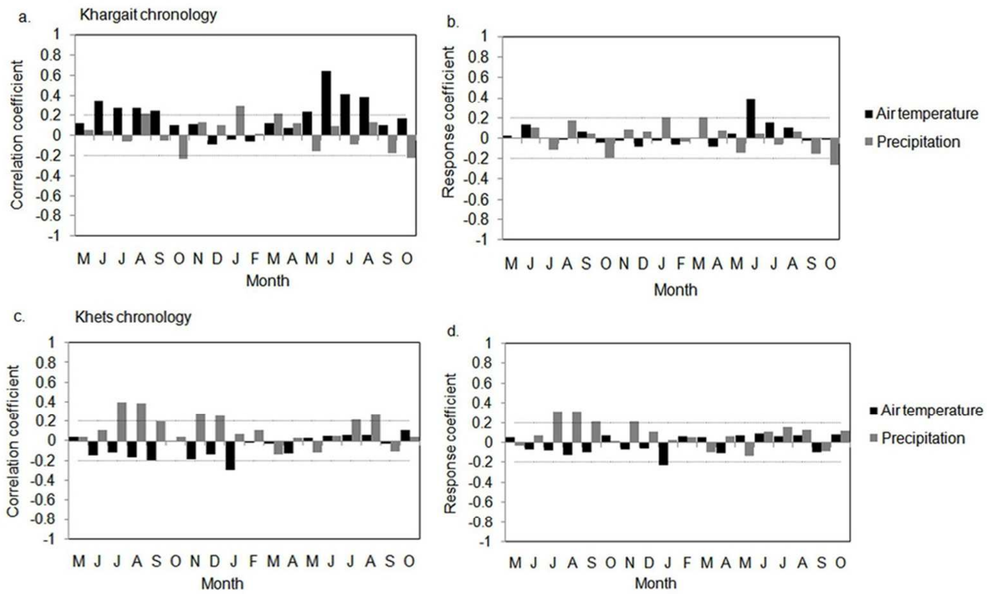

Figure 4

94x58mm (300 x 300 DPI)

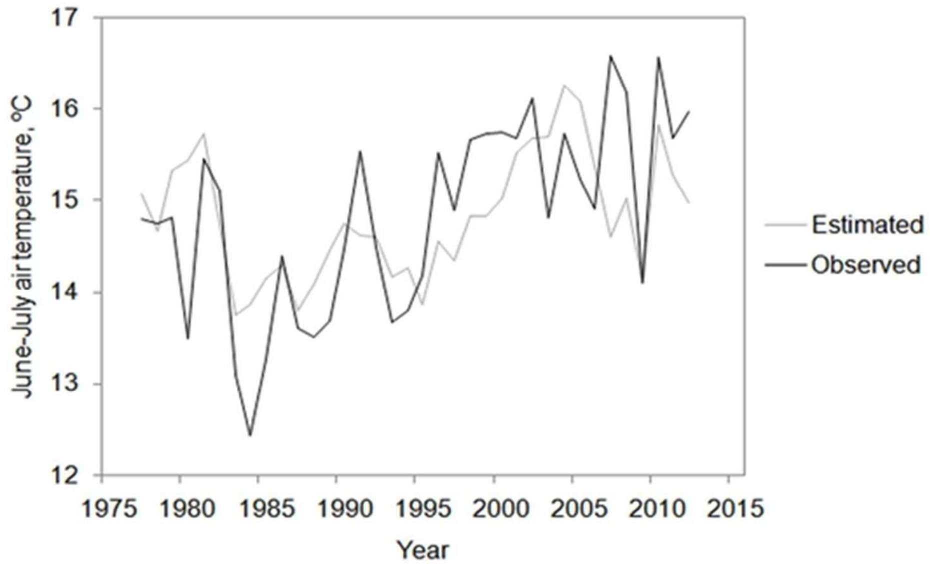

Figure 5

48x29mm (300 x 300 DPI)

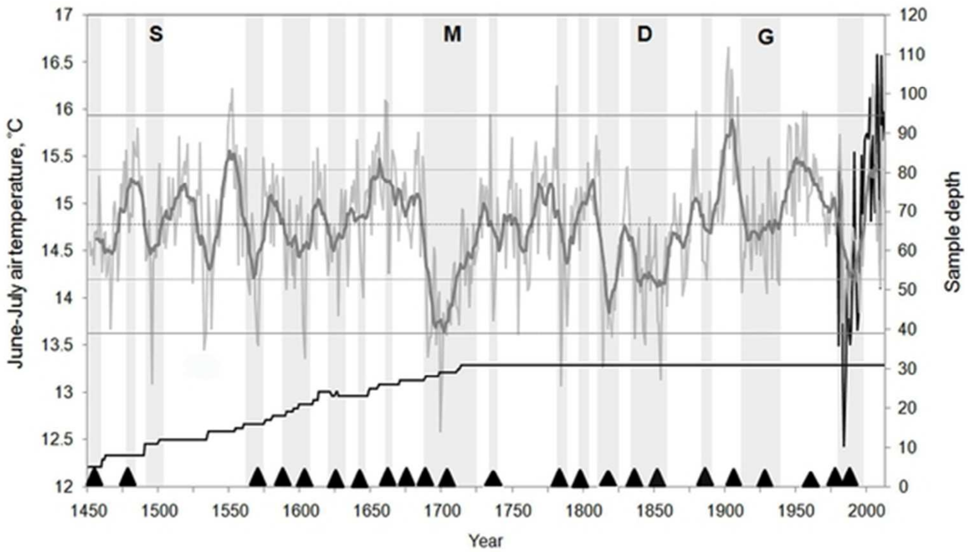

Figure 6

52x30mm (300 x 300 DPI)

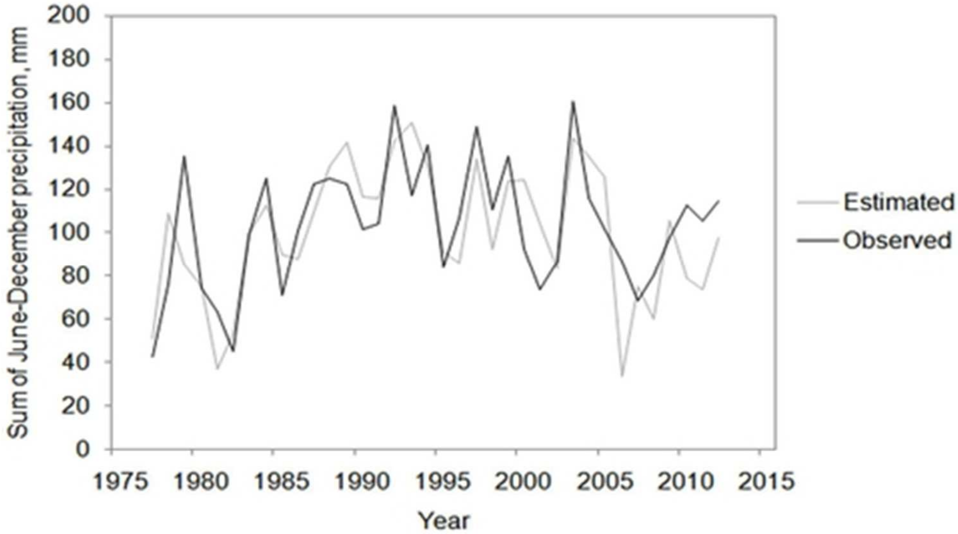

Figure 7

42x23mm (300 x 300 DPI)

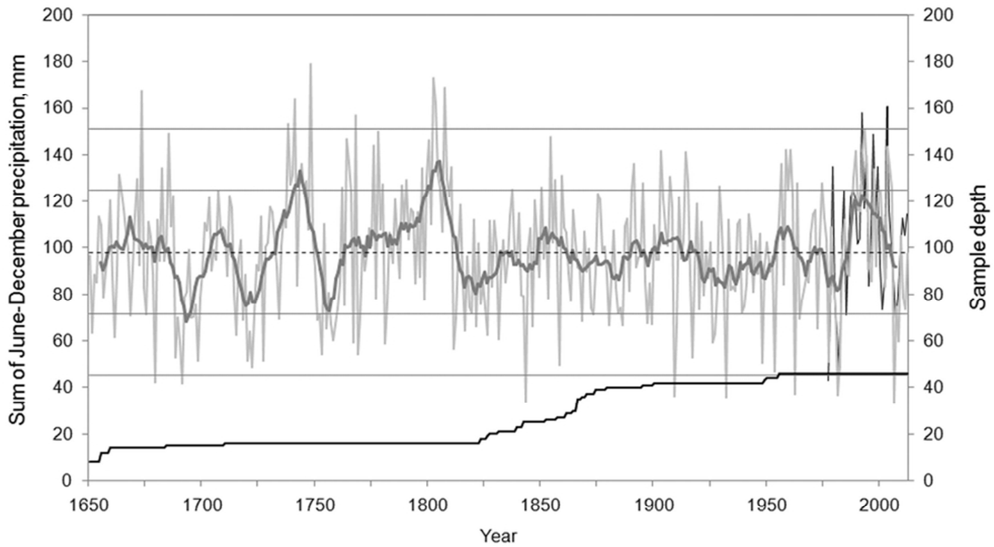

Figure 8

76x54mm (300 x 300 DPI)

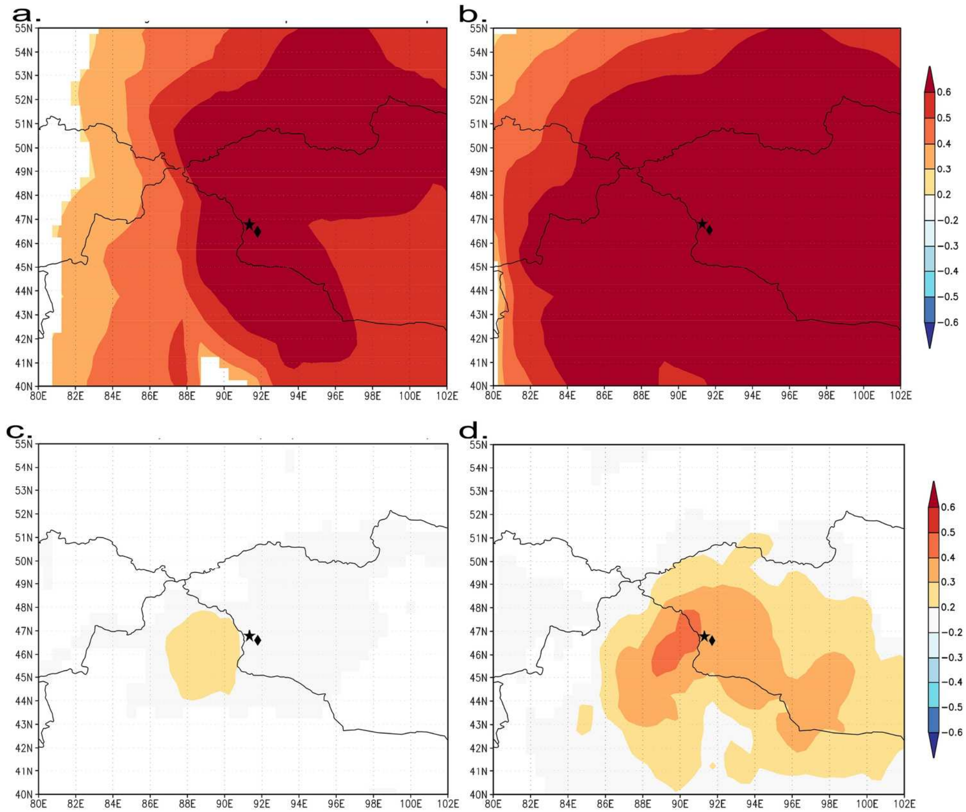

Figure 9

180x180mm (300 x 300 DPI)

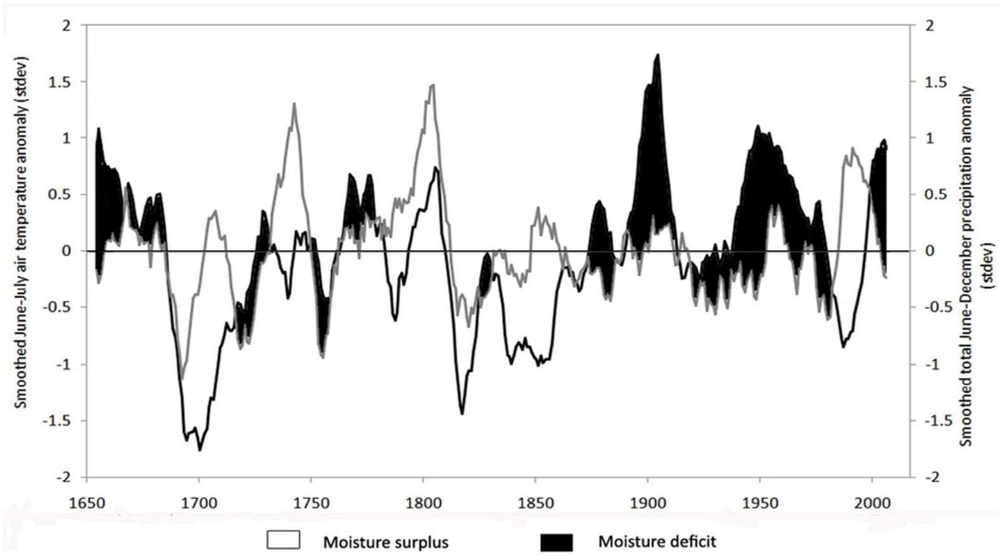

Figure 10

80x53mm (300 x 300 DPI)